# Ground-state properties of quantum rings with a few electrons: Magnetization, persistent current, and spin chirality

Y. Saiga and D. S. Hirashima
*Department of Physics, Nagoya University, Nagoya 464-8602, Japan*

J. Usukura
*Department of Physics, Tokyo University of Science, Tokyo 162-8601, Japan*

(Received 24 June 2006; revised manuscript received 27 November 2006; published 29 January 2007)

Ground-state properties of one-dimensional quantum rings with a few electrons, which interact with each other in the form of $1/r$ Coulomb repulsion, are studied by exact diagonalization. For three electrons, the fully spin-polarized ground state is uniquely realized when the diameter of the ring is sufficiently large. In contrast, for four and five electrons, the fully polarized state never becomes the unique ground state, however large the diameter is. These results can be understood in terms of the multiple-spin exchange. When a perpendicular magnetic field is applied to the ring (i.e., the Aharonov-Bohm flux is introduced), the persistent current occurs, and the spin chirality is finite for a certain value of the flux. The difference between the quantum ring and the circularly arranged quantum dots is also discussed.

DOI: 10.1103/PhysRevB.75.045343 PACS number(s): 73.21.−b, 75.75.+a, 73.23.Ra

## I. INTRODUCTION

Quantum dots[1–3] occupy an important position not only in the field of basic science, but also in the field of nanotechnology. One can change the size of dots from nanometers to microns, and the number of confined electrons one by one. One can also fabricate various shapes of quantum dots with self-assembly methods[4,5] or lithographic techniques.[6–12] By changing the size and shape of dots, and the number of confined electrons, one can control the electronic properties of these quantum nanostructures; this makes quantum dots a unique research subject in basic science as well as an important item in application.

A quantum ring structure[13] is a particularly interesting nanostructure. Both the diameter and the ring width can be separately changed. Furthermore, a magnetic field applied perpendicularly to a ring gives rise to peculiar properties such as a persistent current through Aharonov-Bohm effect.[14] These varieties make quantum rings even more interesting playgrounds for many-body physics and also a strong candidate for a building block of future nanotechnology.

In a previous work,[15] the present authors numerically demonstrated that for three-electron systems, the fully spin-polarized ground state is more likely to be realized in a quantum ring than in a harmonic confinement. In this case, the contribution of multiple-spin exchange was essential.[16] The purposes of the present paper are (1) to extend the previous study to four- and five-electron systems and show that multiple-spin exchange is also essential to determine spin states of the system, and (2) to study the effect of a magnetic field perpendicularly applied to a ring and show that the field not only gives rise to a persistent current, but also has an effect on spin state of the system and indeed induces finite spin chirality.

As for the multiple-spin exchange, it is known that the exchange processes involving odd-number electrons favor ferromagnetism and those involving even-number electrons favor antiferromagnetism.[17] Thus, if electrons are confined in quasi-one-dimensional space, then the multiple-spin exchange (the cyclic exchange) becomes dominant and the difference of the number of electrons by one would lead to qualitative change of the ground-state properties. Namely, it is possible that the physics in a quantum ring including a few electrons is distinct from the Tomonaga-Luttinger liquid in the low density limit. Although one may naively expect that the ground state for even (odd)-number electrons is the spin-singlet (fully polarized) state, the situation is not so simple. In this work, we study roles played by multiple-spin exchanges in few-electron systems in quantum rings of various size. This is the first issue which will be addressed in this paper.

In addition to the number of electrons, application of a perpendicular magnetic field should bring about the diversity of physical properties.[13] A magnetic flux threading a ring (i.e., the Aharonov-Bohm flux) induces a persistent current.[18–21] Without a level crossing in the presence of the field, the periodicity of the persistent current must be the unit flux quantum. However, as we shall see, a level crossing does occur in a magnetic field, which results in a shorter periodicity of the persistent current. The level crossing in a magnetic field is related with the evolution of the total angular momentum and the total spin in the ground state induced by the magnetic field.[22] Besides, in the presence of a field, the spin chirality is expected to appear owing to explicit breaking of time-reversal symmetry. The spin chirality has been discussed from several aspects in condensed matter physics.[23–30] The effects of the chirality in quantum nanostructures are also discussed,[31] but studies of these effects are still premature. Studies of the persistent current and the spin chirality in quantum rings in a magnetic field are then the second issue in this work.

In the present paper, we focus on the structure of a one-dimensional (1D) ring and study (i) the ground-state properties of three-, four-, and five-electron systems without a magnetic field; (ii) the magnetic-field effect on three, four, and five electrons. To this end, the exact-diagonalization method is employed. As a result, we find that, for four and five electrons, the fully polarized state never becomes the unique

 

ground state, however large the size of the ring is. The nature of magnetism (i.e., magnetization) is determined by the effective repulsion between electrons at the same position and is little influenced by the long-range part of the Coulomb repulsion, whereas the Wigner crystal-like states are realized because of the long-range part of the Coulomb repulsion. We also observe features of spin chirality in a quantum ring.

The paper is organized as follows: In the next section, we introduce the model and describe our strategy. In Sec. III, the results of a few electrons in the absence of magnetic field are presented. In Sec. IV, we show the results of the energy spectrum, the persistent current, and the spin chirality in a magnetic field. Section V is devoted to a summary of this study. In the Appendix, we discuss the case of circularly arranged quantum dots, which is compared with the quantum ring.

## II. MODEL

We consider a system of $N$ interacting electrons confined in a 1D quantum ring with circumference $L$. The interaction has the $1/r$ Coulomb type. When a perpendicular magnetic field is applied, the Hamiltonian is given by[20,22]

$$\mathcal{H} = \frac{\hbar^2}{2m_e^*}\sum_{i=1}^{N}\left(-i\frac{\partial}{\partial x_i} - \frac{2\pi}{L}\frac{\Phi}{\Phi_0}\right)^2 + \sum_{\langle ij\rangle}\frac{e^2}{\epsilon d_{ij}}, \tag{1}$$

where $m_e^*$ is the effective electron mass, $\epsilon$ is the dielectric constant, and $d_{ij}=(L/\pi)|\sin[\pi(x_i-x_j)/L]|$ is the chord distance between $x_i$ and $x_j$. The pair $\langle ij\rangle$ takes all the combinations of individual (labeled) electrons. [For $N=3$, we take $(i,j)=(1,2)$, (2,3), and (1,3).] $\Phi$ is the total magnetic flux through the ring, and $\Phi_0$ is the unit flux quantum $h/e$. We neglected the Zeeman coupling of spins to the magnetic field. The Hamiltonian (1) can be rewritten as

$$\mathcal{H}/H^* = \frac{1}{2}\sum_{i=1}^{N}(a_B^*)^2\left(-i\frac{\partial}{\partial x_i} - \frac{2\pi}{L}\frac{\Phi}{\Phi_0}\right)^2 + \sum_{\langle ij\rangle}\frac{1}{d_{ij}/a_B^*}, \tag{2}$$

where

$$a_B^* = \frac{\hbar^2\epsilon}{m_e^* e^2} \tag{3}$$

is the effective Bohr radius, and

$$H^* = \frac{e^2}{\epsilon a_B^*} = \frac{m_e^* e^4}{\epsilon^2\hbar^2} \tag{4}$$

is the effective Hartree. For the material parameter of GaAs, using $\epsilon=12.6$ and $m_e^*=0.067m_e$, we have $a_B^*=9.95$ nm and $H^*=11.48$ meV. The large value of $a_B^*$ (compared with the Bohr radius $a_B=0.0529$ nm) is due to the small effective mass and the large dielectric constant.

Similarly to Ref. 15, we discretize the circle into $N_m$ pieces and consider a Hamiltonian defined on a 1D lattice with $N_m$ lattice points,

$$\mathcal{H}_{\rm lat}/H^* = -\bar{t}\sum_{\ell=1}^{N_m}\sum_{\sigma=\uparrow,\downarrow}\left[\exp\left(i\frac{2\pi a}{L}\frac{\Phi}{\Phi_0}\right)c_{\ell\sigma}^\dagger c_{\ell+1,\sigma} + \text{H.c.}\right] + \sum_{\ell<m}^{N_m}\bar{U}(|\ell-m|)n_\ell n_m + \bar{U}(0)\sum_{\ell=1}^{N_m}n_{\ell\uparrow}n_{\ell\downarrow} + C, \tag{5}$$

where $\bar{t}=(a_B^*/a)^2/2$, $\bar{U}(|\ell-m|)=a_B^*/\tilde{d}_{\ell m}$, $\bar{U}(0)=a_B^*/\tilde{d}_0$, and $C=N(a_B^*/a)^2$. The operator $c_{\ell\sigma}^\dagger$ ($c_{\ell\sigma}$) is the creation (annihilation) operator of an electron with spin $\sigma$ at $\ell$th lattice point, $n_\ell=\Sigma_\sigma n_{\ell\sigma}=\Sigma_\sigma c_{\ell\sigma}^\dagger c_{\ell\sigma}$, and $a=L/N_m$. We require a condition $c_{N_m+1,\sigma}=c_{1\sigma}$ for a ring geometry. In order to avoid the singularity of $1/d_{ij}$ at $x_i=x_j$ in the Hamiltonian (2), we introduced $\tilde{d}_{\ell m}$ as follows:

$$\tilde{d}_{\ell m} = (d_{\ell m}^2 + c^2)^{1/2} = \frac{L}{\pi}\left[\sin^2\left(\frac{\pi a(\ell-m)}{L}\right) + \delta^2\right]^{1/2}, \tag{6}$$

$$\tilde{d}_0 \equiv \tilde{d}_{\ell\ell} = \frac{L\delta}{\pi}. \tag{7}$$

We defined $c$ as $L\delta/\pi$ with fixed $\delta$. Roughly speaking, the value of $\delta$ corresponds to the width of a quantum ring, which permits an electron to pass another electron. We note that the ratio $\bar{U}(0)/\bar{t}$ is proportional to $L$, i.e., $\bar{U}(0)/\bar{t}=2\pi L/(a_B^* N_m^2\delta)$. In the limit $a\to 0$ ($N_m\to\infty$), we expect that the discretized Hamiltonian (5) reduces to the continuous one (2).

In order to explore the effects of long-range part of the Coulomb interaction, we also consider the 1D conventional Hubbard model with on-site Coulomb repulsion given by

$$\mathcal{H}_{\rm Hub} = -t\sum_{\ell=1}^{N_m}\sum_{\sigma=\uparrow,\downarrow}\left[\exp\left(i\frac{2\pi}{N_m}\frac{\Phi}{\Phi_0}\right)c_{\ell\sigma}^\dagger c_{\ell+1,\sigma} + \text{H.c.}\right] + U\sum_{\ell=1}^{N_m}n_{\ell\uparrow}n_{\ell\downarrow}. \tag{8}$$

In our calculations, we set $a_B^*=H^*=\Phi_0=1$. We employ exact diagonalization to investigate the ground-state properties of the models introduced in this section. In order to obtain states in the subspace with total spin $S_{\rm tot}$, we use the projection operator given by[32]

$$P(S_{\rm tot}) = \prod_{S'_{\rm tot}(\neq S_{\rm tot})}\frac{(\boldsymbol{S}_{\rm tot})^2 - S'_{\rm tot}(S'_{\rm tot}+1)}{S_{\rm tot}(S_{\rm tot}+1) - S'_{\rm tot}(S'_{\rm tot}+1)}, \tag{9}$$

where $\boldsymbol{S}_{\rm tot}$ denotes the summation of the spin operator $\boldsymbol{S}_\ell$ over all lattice points $\ell$. In the following, the lowest energy in the subspace with a specified total spin $S_{\rm tot}$ is denoted by $E_0(S_{\rm tot})$.

## III. FEW ELECTRONS IN A QUANTUM RING WITHOUT A MAGNETIC FIELD

In this section, we study a few electrons ($N=3$, 4, and 5) in a 1D ring in the absence of a magnetic field (i.e., $\Phi=0$). For a quantum ring with $\Phi=0$, the $N=3$ case was investi-

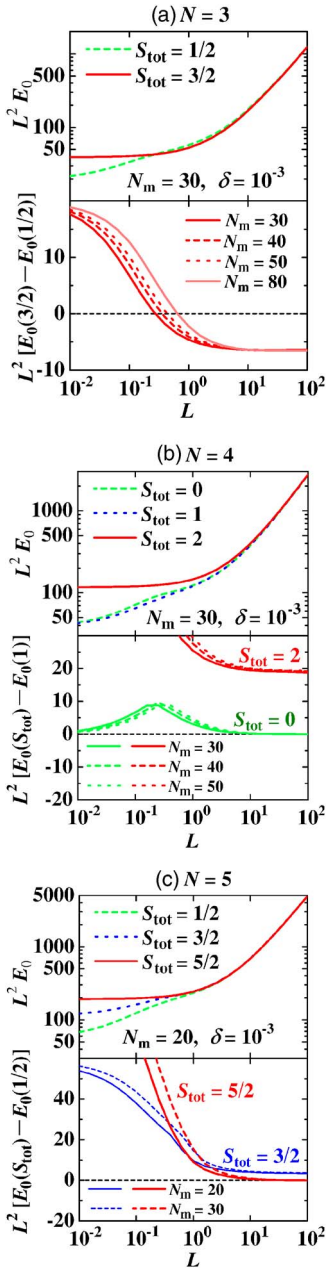


FIG. 1. (Color online) The lowest energies for each total spin and the energy differences as a function of circumference $L$ in the model (5) with $\Phi=0$. (a) $N=3$, (b) $N=4$, (c) $N=5$. The lattice constant is $a=L/N_m$. The effective atomic units are used ($a_B^*=H^*=1$).

gated by means of the stochastic variational method[15] and exact diagonalization.[15,33] The general $N$ case has recently been studied within local-spin-density functional theory.[34] As the study of few-electron systems in the strong coupling region is a difficult task, it is worth studying them with various complementary methods. Here, we present our results for $N=3$, 4, and 5 with exact diagonalization, and make a comparison with the previous studies.[15,33,34] The interpretation of the results in the strong coupling region shall be discussed in terms of multiple-spin exchange.

Figure 1 shows the lowest energies for each total spin (with a fixed $N_m$) and the energy differences as a function of circumference $L$. For a convergence check, we also show the energy differences with various $N_m$. While the energy differences have the weak $N_m$ dependence in the small $L(\sim 10^{-2})$ and large $L(\gtrsim 10)$ regimes, the $N_m$ dependence of the energy differences is somewhat large in the intermediate regime of $L$. Nevertheless, the main feature (such as the presence or absence of level crossing) seems to be unchanged. Thus we believe that the data for $N_m \sim 30$ catch the feature in the continuous limit ($N_m \to \infty$). In the following, we discuss the results with $N_m=20-30$.

From Fig. 1, we find that, irrespective of the number of electrons, the obtained energy has a crossover from $E_0 \propto 1/L^2$ in the small $L$ regime, to $E_0 \propto 1/L$ in the large $L$ regime. This indicates that the kinetic energy is dominant in the weak coupling regime ($L \ll 1$), while the Coulomb interaction is dominant in the strong coupling regime ($L \gg 1$). For $N=3$, the level crossing occurs. Namely, the total spin of the ground state changes from $S_{\rm tot}=1/2$ to $S_{\rm tot}=3/2$ (i.e., maximum possible total spin) with increasing $L$. This feature was observed also in Ref. 15. The spin transition of the ground state has also been seen in a more realistic model.[33] On the other hand, for four and five electrons, states with different $S_{\rm tot}$ tend to be degenerate as $L$ becomes large. In particular, for five electrons, the fully spin-polarized state seems to be almost one of the ground states in a region $L \gtrsim 10$. For all $N$'s, our results on the total spin of the ground state in the intermediate-$L$ regime ($L \sim 1$) are consistent with those obtained with local-spin density functional theory.[34]

In addition to the total spin $S_{\rm tot}$, the total angular momentum $M_{\rm tot}$ is also a good quantum number in the present model (5). For $N=3$, the lowest state within the $S_{\rm tot}=1/2$ subspace has $M_{\rm tot}=1$ in the whole region of $L$ shown in Fig. 1(a), and the lowest state with $S_{\rm tot}=3/2$ is always accompanied by $M_{\rm tot}=0$. These combinations of $S_{\rm tot}$ and $M_{\rm tot}$ are the same as what one expects from the noninteracting case. For $N=4$, the lowest states with $S_{\rm tot}=1$ and $S_{\rm tot}=2$ are accompanied by $M_{\rm tot}=0$ and $M_{\rm tot}=2$, respectively, in the whole region of $L$. However, in the $S_{\rm tot}=0$ subspace, the total angular momentum of the lowest state changes from $M_{\rm tot}=2$ (for $L \leqslant L_c$) to $M_{\rm tot}=0$ (for $L \geqslant L_c$), where $L_c$ is estimated as approximately 0.2. This value of $L_c$ corresponds to the value at which $L^2[E_0(S_{\rm tot}=0)-E_0(S_{\rm tot}=1)]$ has the maximum in the lower panel of Fig. 1(b). For $N=5$, the lowest state within the $S_{\rm tot}=5/2$ subspace always has $M_{\rm tot}=0$; on the other hand, with increasing $L$, we have $M_{\rm tot}=1 \to 0$ with $L_c \simeq 1$ in the $S_{\rm tot}=1/2$ subspace, and $M_{\rm tot}=2 \to 1$ with $L_c \simeq 0.4$ in the $S_{\rm tot}=3/2$ subspace. The values of $M_{\rm tot}$ in larger $L$ for $S_{\rm tot}=1/2$ and 3/2 are distinct from what is predicted from the free picture.

Now let us discuss our results in the light of Herring's argument.[16] Herring showed that the unique ground state of three spin-1/2 fermions confined in a 1D ring is a spin-polarized one when the interaction potential "becomes rapidly infinite as two fermions approach each other." He further argued that even if the repulsion potential is decreased from infinity to a large finite value, the ground state remains to be a fully spin-polarized one. These arguments can be extended to the case of odd number of fermions.[16] In the case of odd number of fermions, one can show that (i) the fully

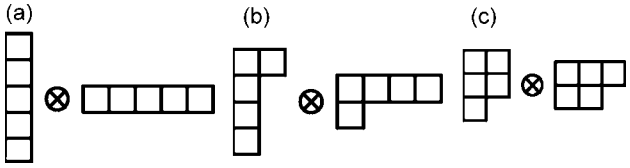


FIG. 2. Possible Young diagrams for $N=5$. In each figure, the diagram on the left (right) hand of the mark $\otimes$ corresponds to the orbital (spin) part of a wave function. A wave function is antisymmetrized with respect to a column, and is symmetrized with respect to a row.

spin-polarized state is one of the ground states, and that (ii) the lowest energy with $S_{\mathrm{tot}}=S_{\mathrm{max}}-1$ is higher than the lowest energy with $S_{\mathrm{tot}}=S_{\mathrm{max}}$, where $S_{\mathrm{max}}$ is given by $N/2$. These statements have been proved via a different method by Aizenman and Lieb.[35]

Let us take the $N=5$ case in a 1D ring as an example. If five particles are distinguishable, the coordinate set of the particles can be expressed as one point in the five-dimensional box where the length of each side is $L$. An actual eigenfunction can be written as a linear combination of $5!=120$ bases in the five-dimensional configuration space. The four-dimensional hyperplanes on which the coordinates of any two of the particles coincide, divide the five-dimensional space into 24 connected regions. Here each region is composed of bases that are transformed with each other under cyclic exchanges. For instance, suppose that $\phi(x_1,x_2,x_3,x_4,x_5)=\phi(12345)$ is a orthonormal basis function belonging to one of the 24 regions. Then, the other four functions generated by cyclic exchanges, $\phi(23451)$, $\phi(34512)$, $\phi(45123)$, and $\phi(51234)$ also belong to the same region. In general, the lowest eigenfunction in the orbital part must be nodeless. However, if the interaction potential becomes rapidly infinite as two particles approach each other, the orbital wave function must vanish on the surface separating the regions that are connected by two-particle exchanges. Under this restriction, a wave function which has the same sign within each region could become the ground-state eigenfunction for odd-number fermions with spin 1/2.[36] Such wave functions are not unique. One is the totally symmetric wave function which has the same sign in all the regions, but the associated spin state is unphysical. Another choice is the wave function that is antisymmetric with respect to coordinate exchange of any two of the particles. Since this wave function is totally antisymmetric, the associated wave function in the spin part should be totally symmetric, leading to the maximum possible total spin $S_{\mathrm{max}}$.

In general, wave functions in many-electron systems can be classified by the Young diagrams. For $N=5$, possible Young diagrams turn out to be limited to three types of the diagrams shown in Fig. 2. The total spins of the diagrams in Figs. 2(a), 2(b), and 2(c) are $S_{\mathrm{tot}}=5/2$, $3/2$, and $1/2$, respectively. The diagram in Fig. 2(a) corresponds to a direct product of the totally antisymmetrized wave function (in the orbital part) and the totally symmetrized wave function (in the spin part), which is one of the ground states as explained in the preceding paragraph. We find that the character of the cyclic permutation in Fig. 2(a) is +1, while that in Fig. 2(b) is −1. The minus sign in the latter case implies that the wave function possesses nodal surfaces interior to a region which is composed of bases with the cyclic order of particles. Thus, the lowest eigenfunction with $S_{\mathrm{tot}}=3/2(=S_{\mathrm{max}}-1)$ necessarily has an energy higher than that with $S_{\mathrm{tot}}=5/2(=S_{\mathrm{max}})$ by a finite amount.

The statements (i) and (ii) should be compared with our results for $N=3$ and 5 with $L\gg 1$, because a large $L$ yields a large repulsion at the same position. In fact, our results do not contradict Herring's argument.

The consistency with Herring's argument implies that the multiple-spin exchange dominantly contributes in our system with large $L$. Since the repulsion between electrons is strong, only the $N$-cyclic exchange would survive as the multiple-spin exchanges. In order to confirm this, we diagonalize a Hamiltonian with only cyclic exchange for each number of electrons. If, for $N=3$, the Hamiltonian is $\mathcal{H}=-(P_{123}+\mathrm{H.c.})$, where $P_{ij\cdots\ell}$ denotes the cyclic permutation of electrons on sites $i,j,\ldots,\ell$, then the eigenvalues are $E=-2$ with $(D_{1/2},D_{3/2})=(0,1)$ and $E=1$ with $(D_{1/2},D_{3/2})=(2,0)$, where $D_{S_{\mathrm{tot}}}$ denotes the number of degeneracies associated with total spin $S_{\mathrm{tot}}$. If the Hamiltonian is $\mathcal{H}=P_{1234}+\mathrm{H.c.}$ for $N=4$, then the eigenvalues are $E=-2$ with $(D_0,D_1,D_2)=(1,1,0)$, $E=0$ with $(D_0,D_1,D_2)=(0,2,0)$, and $E=2$ with $(D_0,D_1,D_2)=(1,0,1)$. If the Hamiltonian is $\mathcal{H}=-(P_{12345}+\mathrm{H.c.})$ for $N=5$, then the eigenvalues are $E=-2$ with $(D_{1/2},D_{3/2},D_{5/2})=(1,0,1)$, $E\simeq -0.618$ with $(D_{1/2},D_{3/2},D_{5/2})=(2,2,0)$, and $E\simeq 1.618$ with $(D_{1/2},D_{3/2},D_{5/2})=(2,2,0)$. These results on degeneracy are consistent with the results of Fig. 1 for large $L$ in all cases of number of electrons.

One may ask why the ground state for $N=4$ is a triplet state in the whole region of $L$ [see Fig. 1(b)]. For $L\ll 1$ (the weak-coupling region), the triplet ground state can be understood as a result of Hund's rule. Namely, the present problem can be effectively mapped into a two-electron problem in two degenerate states, because the other two electrons form a singlet pair in the lowest state of the band dispersion. The consequence is that the presence of repulsive interaction between two electrons makes a triplet state lower in energy than a singlet state. On the other hand, when one starts from the strong coupling limit and considers the region with $L\gg 1$, one may deal with the Hamiltonian having the four-cyclic exchange [Eq. (24) with $\Phi=0$] and the (small) antiferromagnetic exchange between nearest-neighbor spins (i.e., the two-spin exchange). Apparently, the perturbation due to the two-spin exchange seems to stabilize a singlet state, but this is not true in the present case. With only the four-cyclic exchange (i.e., an unperturbed Hamiltonian), a singlet state and a triplet one are degenerate as the ground states, as seen in the preceding paragraph. With use of a representation in real space, the singlet state and the triplet one are given by

$$|\Psi_0^{(4)}(S_{\mathrm{tot}}=0)\rangle=\tfrac{1}{2}(|\uparrow\uparrow\downarrow\downarrow\rangle-|\uparrow\downarrow\downarrow\uparrow\rangle+|\downarrow\downarrow\uparrow\uparrow\rangle-|\downarrow\uparrow\uparrow\downarrow\rangle) \tag{10}$$

and

$$|\Psi_0^{(4)}(S_{\rm tot}=1)\rangle = \frac{1}{\sqrt{2}}(|\uparrow\downarrow\uparrow\downarrow\rangle - |\downarrow\uparrow\downarrow\uparrow\rangle), \tag{11}$$

respectively. The singlet state $|\Psi_0^{(4)}(S_{\rm tot}=0)\rangle$ is nothing but a direct product of two "diagonal" singlet pairs, not including nearest-neighbor singlet pairs, i.e., $[1,3]\otimes[2,4]$ where

$$[i,j] = |\overset{i\ j}{\uparrow\downarrow}\rangle - |\overset{i\ j}{\downarrow\uparrow}\rangle, \tag{12}$$

for sites $i,j$. Meanwhile, for only the antiferromagnetic exchange between nearest-neighbor spins, the singlet ground state is given by

$$|\Psi_0^{(2)}(S_{\rm tot}=0)\rangle = \frac{1}{\sqrt{12}}(|\uparrow\uparrow\downarrow\downarrow\rangle + |\uparrow\downarrow\downarrow\uparrow\rangle + |\downarrow\downarrow\uparrow\uparrow\rangle + |\downarrow\uparrow\uparrow\downarrow\rangle - 2|\uparrow\downarrow\uparrow\downarrow\rangle - 2|\downarrow\uparrow\downarrow\uparrow\rangle). \tag{13}$$

Note that this state is equivalent to a state $-[1,2]\otimes[3,4]+[2,3]\otimes[1,4]$. It is evident that the state $|\Psi_{\rm GS}^{(2)}(S_{\rm tot}=0)\rangle$ is orthogonal to the state $|\Psi_{\rm GS}^{(4)}(S_{\rm tot}=0)\rangle$, although both states are singlet. Thus, the energy of the singlet state $|\Psi_{\rm GS}^{(4)}(S_{\rm tot}=0)\rangle$ for only the four-cyclic exchange is never affected by introduction of the two-spin exchange. In contrast, the energy of the triplet state $|\Psi_0^{(4)}(S_{\rm tot}=1)\rangle$ is lowered as a consequence of the first-order perturbation due to the two-spin exchange. That is why a triplet state is also stabilized in the region with $L \gg 1$.

Next, let us consider whether the long-range part of the Coulomb interaction influences the nature of the magnetism. To answer this question, we also study the 1D conventional Hubbard model with *only* on-site Coulomb repulsion. Figure 3 shows the lowest energies for each total spin and the energy differences as a function of $U/t$, in cases of $N=3$, 4, and 5. We find that, for each $N$, the $U/t$ dependence of the energy differences is very similar to the $L$ dependence of the energy differences in Fig. 1, although the absolute values in Figs. 3 and 1 are largely different because of the difference in the energy unit. Thus we can conclude that the long-range part of the Coulomb interaction hardly influences the nature of the magnetism. The long-range part would determine whether the Wigner-crystal state is realized or not.

Thus far, we have kept the continuous space on a ring in mind, although our actual calculation treats a discretized system. Away from a continuous ring (i.e., a quantum ring), we can also consider a system of the circularly arranged quantum dots. The results in this case, which are given in the Appendix, are distinctly different from those in a continuous ring.

## IV. FEW ELECTRONS IN A QUANTUM RING WITH A MAGNETIC FIELD

A magnetic field applied perpendicularly to the ring is expected to induce a persistent current and spin chirality. The persistent current is given by

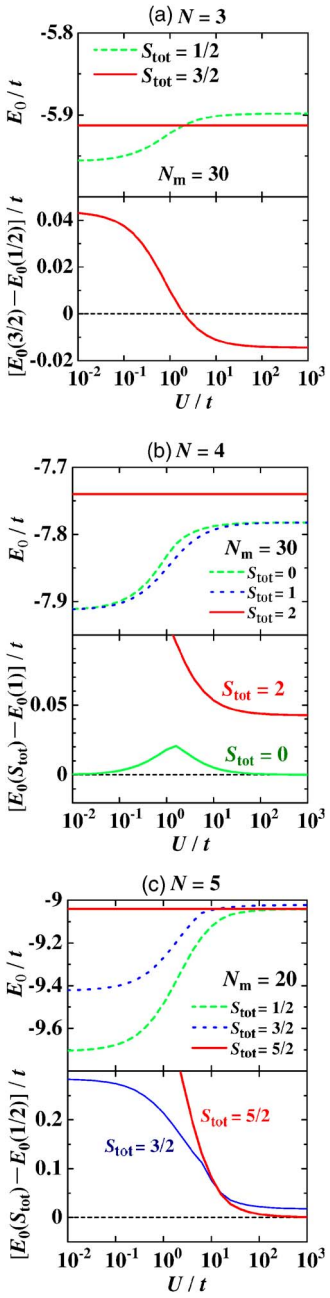


FIG. 3. (Color online) The lowest energies for each total spin and the energy differences as a function of $U/t$ in the 1D Hubbard model. (a) $N=3$, (b) $N=4$, (c) $N=5$.

$$j_p = -\frac{\partial E_0(\bar{S}_{\rm tot};\Phi)}{\partial\Phi}, \tag{14}$$

where $E_0(S_{\rm tot};\Phi)$ denotes the lowest energy in the presence of magnetic flux $\Phi$ in the subspace with total spin $S_{\rm tot}$. $\bar{S}_{\rm tot}$ is chosen so that $E_0(S_{\rm tot};\Phi)$ is the lowest among $S_{\rm tot}$'s at a fixed $\Phi$. The spin chirality can be defined for at least three electrons. Here, we consider the *total* spin chirality in the continuous space, which is given by

$$\chi_{\mathrm{ch,tot}} = \int\int\int_{x_1<x_2<x_3} dx_1 dx_2 dx_3 \langle T_{123} \rangle, \tag{15}$$

where $T_{123}=\boldsymbol{S}(x_1)\cdot\boldsymbol{S}(x_2)\times\boldsymbol{S}(x_3)$, and $\boldsymbol{S}(x_i)$ is the spin operator at $x_i$. $\langle\cdots\rangle$ denotes the expectation value in the lowest state at a fixed $\Phi$. In the Hamiltonian (5) on a discrete lattice, we use the following formula:

$$\chi_{\mathrm{ch,tot}} = \sum_{i<j<\ell} \chi_{\mathrm{ch}}(ij\ell;\bar{S}_{\mathrm{tot}};\Phi), \tag{16}$$

where $\chi_{\mathrm{ch}}(ij\ell;S_{\mathrm{tot}};\Phi)$ is the *local* spin chirality given by

$$\chi_{\mathrm{ch}}(ij\ell;S_{\mathrm{tot}};\Phi) = \langle \Psi_0(S_{\mathrm{tot}};\Phi)|\boldsymbol{S}_i\cdot\boldsymbol{S}_j\times\boldsymbol{S}_\ell|\Psi_0(S_{\mathrm{tot}};\Phi)\rangle, \tag{17}$$

where $|\Psi_0(S_{\mathrm{tot}};\Phi)\rangle$ denotes the lowest state in the presence of flux $\Phi$ in the subspace with total spin $S_{\mathrm{tot}}$. The lattice points $i$, $j$, and $\ell$ can take the values of the range $[1,N_m]$. Figures 4, 5, and 6 show the energy spectrum at each total spin, the persistent current and the total spin chirality for $N=3$, 4, and 5, respectively. We note that similar results on the energy spectra for $N=3$ and 4 have been obtained in the previous study.[37] In general, the energy spectrum is symmetric about $\Phi=0.5$, and both the persistent current and the spin chirality are antisymmetric about $\Phi=0.5$.

First, let us see the results for $N=3$. For $L=0.1$, the level crossing does not occur between the lowest $S_{\mathrm{tot}}=1/2$ state and the lowest $S_{\mathrm{tot}}=3/2$ state over the whole range of $\Phi$. For $L=1$ and 10, on the other hand, the level crossing of the states with different $S_{\mathrm{tot}}$ does occur at a finite value of $\Phi$; a finite magnetic field depolarizes the system.[38] With increasing $\Phi$ from 0 to 1, the total angular momentum $M_{\mathrm{tot}}$ and the total spin $S_{\mathrm{tot}}$ in the ground state are evolved as $(M_{\mathrm{tot}},S_{\mathrm{tot}})=(1,1/2)\rightarrow(2,1/2)$ for $L=0.1$; $(M_{\mathrm{tot}},S_{\mathrm{tot}})=(0,3/2)\rightarrow(1,1/2)\rightarrow(2,1/2)\rightarrow(3,3/2)$ for $L=1$ and 10. The latter result is consistent with the evolution obtained in a recent study by Liu, Bao, and Shi,[22] who treated the strong coupling region ($L\gtrsim 30$ in our notation). The feature of level crossing affects the $\Phi$ dependence of the persistent current. The amplitude of persistent current becomes small with increasing $L$. We note that, for $L=0.1$, a finite amount of persistent current emerges even at infinitesimal $\Phi$.[39] This is related to the fact that $M_{\mathrm{tot}}$ is nonzero in the ground state. A periodicity of the persistent current becomes short $(\Phi_0/3)$ for a large $L$. This behavior, which can be generalized to the $\Phi_0/N$ periodicity for $N$ electrons, has been obtained in previous theoretical studies;[13,37] the shortness of periodicity has been observed by an experiment.[10] We find that the total spin chirality is (visibly) finite for a certain range of $\Phi$ depending on $L$, and that the finite chirality is almost constant. The constant values are $|\chi_{\mathrm{ch,tot}}|\simeq 0.354$ for $L=0.1$, $|\chi_{\mathrm{ch,tot}}|\simeq 0.431$ for $L=1$, and $|\chi_{\mathrm{ch,tot}}|\simeq 0.433$ for $L=10$. The total spin chirality vanishes when the ground state has the maximum possible total spin (i.e., $S_{\mathrm{tot}}=S_{\mathrm{max}}=3/2$). In this case, the local spin chirality also vanishes.

Next, let us observe the results for $N=4$ and 5. Figures 5 and 6 imply that for $N=4$ and 5, the state with $S_{\mathrm{tot}}=S_{\mathrm{max}}$ never becomes the unique ground state at any flux $\Phi$. With increasing $\Phi$ from 0 to 1, the set of $(M_{\mathrm{tot}},S_{\mathrm{tot}})$ in the ground state is evolved as $(M_{\mathrm{tot}},S_{\mathrm{tot}})=(0,1)\rightarrow(2,0)\rightarrow(4,1)$ for $N=4$ with $L=0.1$; $(M_{\mathrm{tot}},S_{\mathrm{tot}})=(0,1)\rightarrow(1,1)\rightarrow(2,0)\rightarrow(3,1)\rightarrow(4,1)$ for $N=4$ with $L=1$ and 10; $(M_{\mathrm{tot}},S_{\mathrm{tot}})=(1,1/2)\rightarrow(2,3/2)\rightarrow(3,3/2)\rightarrow(4,1/2)$ for $N=5$ with $L=1$. The persistent current has a jump at several values of $\Phi$ where the level crossing occurs in the energy spectra. For $N=4$ with

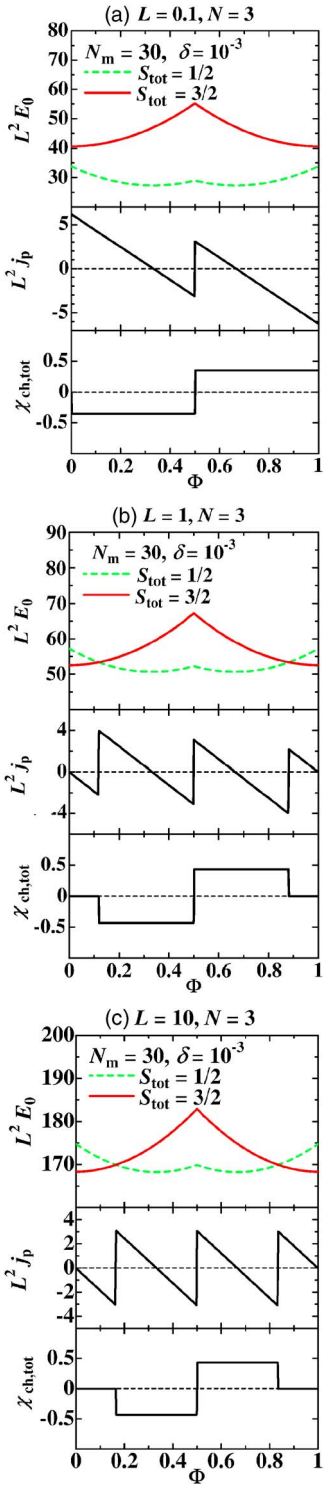


FIG. 4. (Color online) The lowest energies ($E_0$) at each total spin, persistent current ($j_p$) and total spin chirality ($\chi_{\mathrm{ch,tot}}$), as a function of flux ($\Phi$) in the model (5). $N=3$.

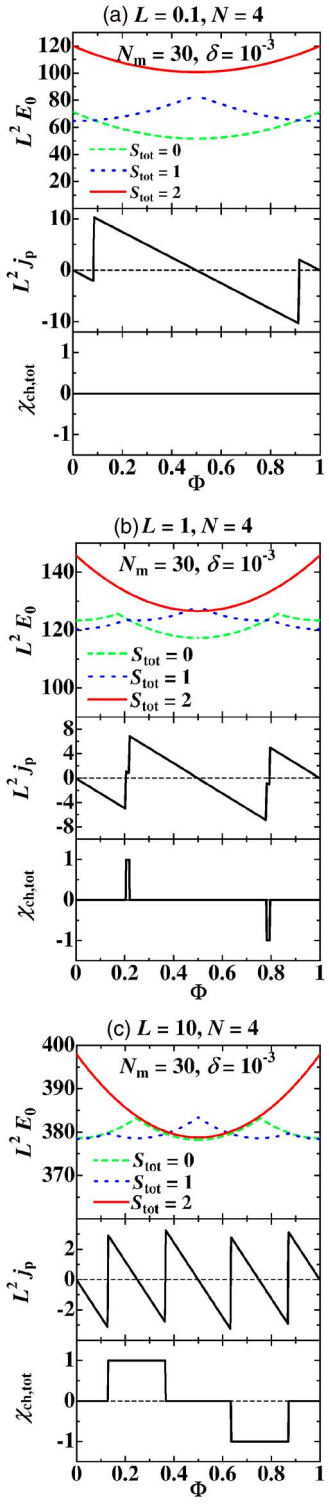


FIG. 5. (Color online) The lowest energies ($E_0$) at each total spin, persistent current ($j_p$) and total spin chirality ($\chi_{\mathrm{ch,tot}}$), as a function of flux ($\Phi$) in the model (5). $N=4$.

$L=10$, the periodicity of persistent current becomes $\Phi_0/4$.[13,37] We again observe the constant $\chi_{\mathrm{ch,tot}}$ for a certain range of $\Phi$. The constant values are $|\chi_{\mathrm{ch,tot}}| \simeq 0.993$ for $N=4$ with $L=1$, and $|\chi_{\mathrm{ch,tot}}| \simeq 1.00$ for $N=4$ with $L=10$. For $N=5$ with $L=1$, we have $\chi_{\mathrm{ch,tot}} \simeq 0.585$ in the range $0<\Phi \lesssim 0.444$, and $\chi_{\mathrm{ch,tot}} \simeq -0.403$ in the range $0.444 \lesssim \Phi < 0.5$. In

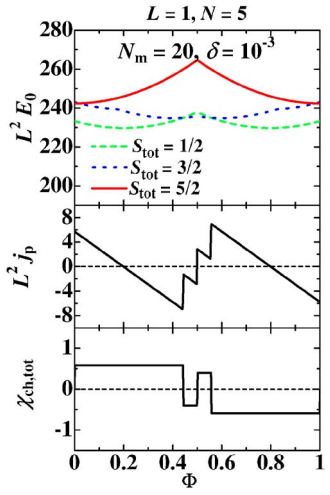


FIG. 6. (Color online) The lowest energies ($E_0$) at each total spin, persistent current ($j_p$) and total spin chirality ($\chi_{\mathrm{ch,tot}}$), as a function of flux ($\Phi$) in the model (5). $N=5$.

contrast to the $N=3$ case, there are the ranges of $\Phi$ where $\chi_{\mathrm{ch,tot}}$ (almost) vanishes in spite of the ground state having $S_{\mathrm{tot}} < S_{\mathrm{max}}$. For example, in case of $N=4$ with $L=1$, we obtain $|\chi_{\mathrm{ch,tot}}| \lesssim 10^{-5}$ in the range $0<\Phi \lesssim 0.206$, and $|\chi_{\mathrm{ch,tot}}| < 10^{-15}$ in the range $0.220 \lesssim \Phi \lesssim 0.5$. This point will be discussed later.

The fact that the local spin chirality vanishes for $S_{\mathrm{tot}} = S_{\mathrm{max}}$ can be proved as follows:[40] For the fully spin-polarized state, wave functions $|S_{\mathrm{tot}}; S^z_{\mathrm{tot}}\rangle$, which have $(N+1)$-fold degeneracy, are written by

$$|S_{\mathrm{tot}} = S_{\mathrm{max}}; S^z_{\mathrm{tot}} = N/2 - m\rangle \propto (S^-_{\mathrm{tot}})^m |S_{\mathrm{tot}} = S_{\mathrm{max}}; S^z_{\mathrm{tot}} = S_{\mathrm{max}}\rangle, \tag{18}$$

where $S^-_{\mathrm{tot}}$ denotes the summation of the spin-lowering operator over all lattice points, and $m=0,1,\ldots,N$. On the other hand, the operator $\boldsymbol{S}_i \cdot \boldsymbol{S}_j \times \boldsymbol{S}_\ell$ with three different lattice points $(i \neq j \neq \ell)$ can be expressed as

$$\begin{aligned} \boldsymbol{S}_i \cdot \boldsymbol{S}_j \times \boldsymbol{S}_\ell &= S^x_i (S^y_j S^z_\ell - S^z_j S^y_\ell) + S^y_i (S^z_j S^x_\ell - S^x_j S^z_\ell) \\ &\quad + S^z_i (S^x_j S^y_\ell - S^y_j S^x_\ell) \\ &= \frac{i}{2}[(S^+_i S^-_j - S^-_i S^+_j) S^z_\ell + (S^+_\ell S^-_i - S^-_\ell S^+_i) S^z_j \\ &\quad + (S^+_j S^-_\ell - S^-_j S^+_\ell) S^z_i]. \end{aligned} \tag{19}$$

By using this expression, we can check that

$$[S^-_{\mathrm{tot}}, \boldsymbol{S}_i \cdot \boldsymbol{S}_j \times \boldsymbol{S}_\ell] = 0$$

and

$$\boldsymbol{S}_i \cdot \boldsymbol{S}_j \times \boldsymbol{S}_\ell |S_{\mathrm{tot}} = S_{\mathrm{max}}; S^z_{\mathrm{tot}} = S_{\mathrm{max}}\rangle = 0.$$

From these facts, we have

$$\begin{aligned}\boldsymbol{S}_i \cdot \boldsymbol{S}_j \times \boldsymbol{S}_\ell | S_{\mathrm{tot}} = S_{\max}; S^z_{\mathrm{tot}} = N/2 - m\rangle \\ \propto \boldsymbol{S}_i \cdot \boldsymbol{S}_j \times \boldsymbol{S}_\ell (S^-_{\mathrm{tot}})^m | S_{\mathrm{tot}} = S_{\max}; S^z_{\mathrm{tot}} = S_{\max}\rangle \\ = (S^-_{\mathrm{tot}})^m \boldsymbol{S}_i \cdot \boldsymbol{S}_j \times \boldsymbol{S}_\ell | S_{\mathrm{tot}} = S_{\max}; S^z_{\mathrm{tot}} = S_{\max}\rangle \\ = 0. \qquad (20)\end{aligned}$$

Thus, we have proved that at any $\Phi$, $\chi_{\mathrm{ch}}(ij\ell; S_{\max}; \Phi)=0$ for all $i,j,\ell$. We note that this result is independent of the spatial dimension. In fact, the local spin chirality vanishes for the ground state with $S_{\mathrm{tot}}=S_{\max}$ in the $U\to\infty$ Hubbard model with magnetic flux perpendicular to a square lattice.[30]

Next, let us derive the effective Hamiltonian in the strong coupling limit in the presence of magnetic field.[28,41] For $N=3$, a clockwise-cyclic permutation of the particles on sites (1,2,3) yields

$$P_{13}P_{12} = \tfrac{1}{4} + \boldsymbol{S}_1 \cdot \boldsymbol{S}_2 + \boldsymbol{S}_2 \cdot \boldsymbol{S}_3 + \boldsymbol{S}_3 \cdot \boldsymbol{S}_1 - 2i\boldsymbol{S}_1 \cdot \boldsymbol{S}_2 \times \boldsymbol{S}_3. \qquad (21)$$

We have used $P_{ij}=2\boldsymbol{S}_i\cdot\boldsymbol{S}_j+1/2$. The coefficient in this case is given by $J\exp(i2\pi\Phi)$. A counterclockwise-cyclic permutation corresponds to the complex conjugate of Eq. (21), which yields

$$P_{12}P_{13} = \tfrac{1}{4} + \boldsymbol{S}_1 \cdot \boldsymbol{S}_2 + \boldsymbol{S}_2 \cdot \boldsymbol{S}_3 + \boldsymbol{S}_3 \cdot \boldsymbol{S}_1 + 2i\boldsymbol{S}_1 \cdot \boldsymbol{S}_2 \times \boldsymbol{S}_3. \qquad (22)$$

The coefficient in this case is given by $J\exp(-i2\pi\Phi)$. By summing Eqs. (21) and (22), we have

$$\begin{aligned}\mathcal{H}_{\mathrm{eff}} = 2J\cos(2\pi\Phi)\left(\tfrac{1}{4} + \boldsymbol{S}_1 \cdot \boldsymbol{S}_2 + \boldsymbol{S}_2 \cdot \boldsymbol{S}_3 + \boldsymbol{S}_3 \cdot \boldsymbol{S}_1\right) \\ + 4J\sin(2\pi\Phi)\boldsymbol{S}_1 \cdot \boldsymbol{S}_2 \times \boldsymbol{S}_3. \qquad (23)\end{aligned}$$

The exchange constant $J$ is taken to be negative so that it favors ferromagnetism for $\Phi=0$.[17] The second term is precisely the contribution of the spin chirality. From this Hamiltonian, we can naturally understand the vanishing spin chirality at $\Phi=0$ and 0.5. All the eigenvalues in the Hamiltonian (23) are shown in Fig. 7. We confirm that the $\Phi$ dependence of the lowest energy for $L=10$ (shown in the bottom figure of Fig. 4) is reproduced by the effective Hamiltonian (23). In particular, the value of $\Phi$ at which the depolarization appears is given by 0.166 ($\sim 1/6$). This means that the depolarization is not just determined by the change in the sign of the exchange interaction, and that the spin-chirality term also contributes the depolarization.

Similarly, for $N=4$, we obtain

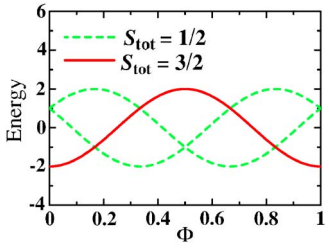


FIG. 7. (Color online) The $\Phi$ dependence of all the eigenvalues in the effective Hamiltonian (23) with $J=-1$ for $N=3$.

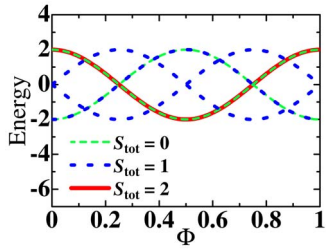


FIG. 8. (Color online) The $\Phi$ dependence of all the eigenvalues in the effective Hamiltonian (24) with $J=-1$ for $N=4$.

$$\begin{aligned}\mathcal{H}_{\mathrm{eff}} = -J\exp(i2\pi\Phi)\left(2\boldsymbol{S}_1 \cdot \boldsymbol{S}_2 + \tfrac{1}{2}\right)\left(2\boldsymbol{S}_2 \cdot \boldsymbol{S}_3 + \tfrac{1}{2}\right) \\ \times \left(2\boldsymbol{S}_3 \cdot \boldsymbol{S}_4 + \tfrac{1}{2}\right) + \mathrm{H.c.} \\ = -J\cos(2\pi\Phi)\Big[\tfrac{1}{4} + \boldsymbol{S}_1 \cdot \boldsymbol{S}_2 + \boldsymbol{S}_2 \cdot \boldsymbol{S}_3 + \boldsymbol{S}_3 \cdot \boldsymbol{S}_4 \\ + \boldsymbol{S}_4 \cdot \boldsymbol{S}_1 + \boldsymbol{S}_1 \cdot \boldsymbol{S}_3 + \boldsymbol{S}_2 \cdot \boldsymbol{S}_4 - 4(\boldsymbol{S}_1 \cdot \boldsymbol{S}_3)(\boldsymbol{S}_2 \cdot \boldsymbol{S}_4) \\ + 4(\boldsymbol{S}_1 \cdot \boldsymbol{S}_2)(\boldsymbol{S}_3 \cdot \boldsymbol{S}_4) + 4(\boldsymbol{S}_2 \cdot \boldsymbol{S}_3)(\boldsymbol{S}_4 \cdot \boldsymbol{S}_1)\Big] \\ - 2J\sin(2\pi\Phi)(\boldsymbol{S}_1 \cdot \boldsymbol{S}_2 \times \boldsymbol{S}_3 + \boldsymbol{S}_2 \cdot \boldsymbol{S}_3 \times \boldsymbol{S}_4 \\ + \boldsymbol{S}_1 \cdot \boldsymbol{S}_3 \times \boldsymbol{S}_4 + \boldsymbol{S}_1 \cdot \boldsymbol{S}_2 \times \boldsymbol{S}_4). \qquad (24)\end{aligned}$$

As in the case of $N=3$, we encounter the spin-chirality term in the effective Hamiltonian. Again, the contribution of the spin chirality vanishes at $\Phi=0$ and 0.5. In Fig. 8, we show all the eigenvalues in the effective Hamiltonian (24). For $\Phi=0$, the $S_{\mathrm{tot}}=0$ state and the $S_{\mathrm{tot}}=1$ state are degenerate in the lowest energy, and the $S_{\mathrm{tot}}=0$ state and the $S_{\mathrm{tot}}=2$ state are degenerate in the highest energy; these degeneracies are never lifted by the presence of $\Phi$. The results in the effective Hamiltonian reproduce the $\Phi$ dependence of the lowest energy and its (near) degeneracy for $L=10$, which are shown in the bottom figure of Fig. 5.

The results on the spin chirality for $N=4$ (Fig. 5) show that there are the values of $\Phi$ where $\chi_{\mathrm{ch,tot}}$ (almost) vanishes even when the total spin of the lowest state is less than $S_{\max}$. In this case, the local spin chirality has a small but finite value. To see it, we show the local spin chirality given by $\chi_{\mathrm{ch}}(i=1,j,\ell;\bar{S}_{\mathrm{tot}};\Phi)$ in Fig. 9 ($N=3$ with $L=1$) and Fig. 10 ($N=4$ with $L=1$). Note that the local spin chirality is antisymmetric with respect to exchange of $j$ and $\ell$ [see Eq. (17)]. For $N=3$, the local spin chirality has a peak at $(j-1,\ell-1)=(20,10)$. This means that the spin chirality tends to take a large value among three points separated by the same dis-

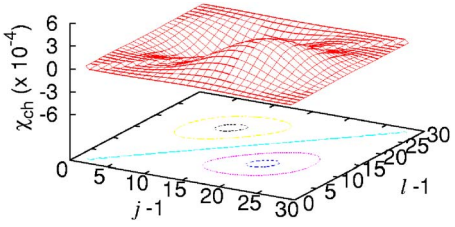


FIG. 9. (Color online) Local spin chirality given by $\chi_{\mathrm{ch}}$ ($i=1,j,\ell$; $\bar{S}_{\mathrm{tot}}=1/2$; $\Phi=0.3$) for $N=3$, $L=1$, $N_m=30$, and $\delta=10^{-3}$. The total chirality $\chi_{\mathrm{ch,tot}}$ is $\chi_{\mathrm{ch,tot}}=-0.431$.

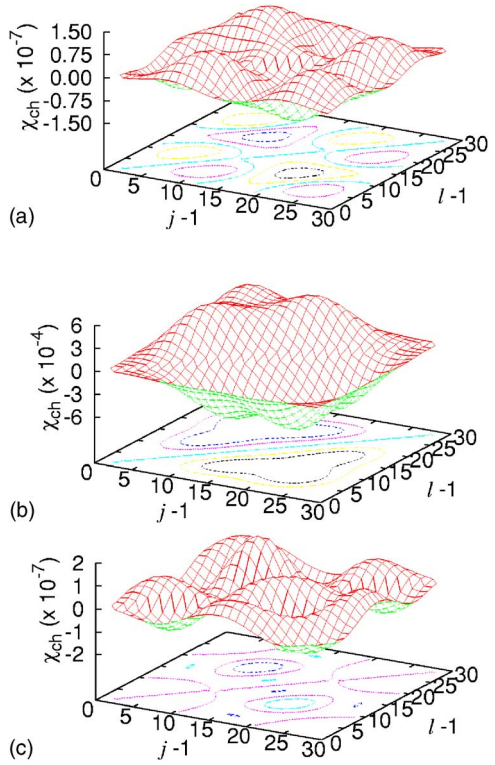


FIG. 10. (Color online) Local spin chirality given by $\chi_{\mathrm{ch}}$ $(i=1,j,\ell;\bar{S}_{\mathrm{tot}};\Phi)$. $N=4$, $L=1$, $N_m=30$, and $\delta=10^{-3}$. (Top) $\bar{S}_{\mathrm{tot}}=1$, $\Phi=0.1$, and $\chi_{\mathrm{ch,tot}}=-1.48\times10^{-5}$; (middle) $\bar{S}_{\mathrm{tot}}=1$, $\Phi=0.21$, and $\chi_{\mathrm{ch,tot}}=0.993$; (bottom) $\bar{S}_{\mathrm{tot}}=0$, $\Phi=0.3$, and $|\chi_{\mathrm{ch,tot}}|<10^{-15}$.

tance $(\sim L/3)$ on a ring. The tendency is plausible because three electrons are likely to be distributed with the same distance separation $(\sim L/3)$. For $N=4$, the situation is more complicated, and a "spin-chirality density wave" emerges depending on the values of $\Phi$, as seen in Fig. 10. When the total spin chirality is finite (in case of the middle figure in Fig. 10), we find that the local spin chirality has the same sign in the region with $j<\ell$ (or $j>\ell$). The distribution of local spin chirality has three peaks at $(j-1,\ell-1)=(7,14)$, (7,23), and (16,23). This distribution almost corresponds to the electron distribution (the three-point charge correlation) which shows that four electrons tend to be distributed with the same distance separation $(\sim L/4)$. In contrast, when the total spin chirality (almost) vanishes (in cases of the top and bottom figures in Fig. 10), the local spin chirality changes its sign in the region with $j<\ell$. The local spin chirality takes the maximum value at $(j-1,\ell-1)=(10,20)$. This indicates that the spin chirality tends to take a large value among three points separated by the same distance $(\sim L/3)$, which is incommensurate with the four-electron distribution. As the diameter of the ring becomes large, the tendency of incommensurability weakens and the spin chirality commensurate with the electron distribution becomes dominant. In fact, for $L=10$, the region of $\Phi$ with large values of the total spin chirality is extended compared with the case of $L=1$, as seen in Fig. 5.

We have revealed that the spin chirality can be present in quantum rings with a finite magnetic field. The spin chirality has some applicability. The degeneracy of states with $S_{\mathrm{tot}}<S_{\mathrm{max}}$ at zero magnetic field is lifted by the presence of both the local spin chirality and the Zeeman term, namely, by application of a perpendicular magnetic field. (Note that we have not included the Zeeman term in this study because the effect is trivial.) This can be utilized for the splitting between the encoded basis states of the qubit in the field of quantum computation.[31] Another applicability is to utilize quantum rings as controllable generators with spin chirality. In fact, it has been discussed that the anomalous Hall effect in a frustrated ferromagnet is explainable by the presence of the spin

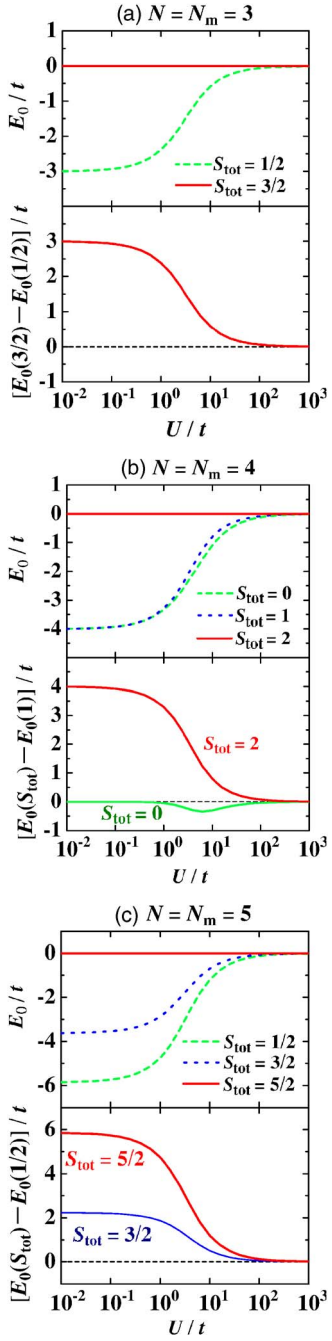


FIG. 11. (Color online) The lowest energies for each total spin and the energy differences as a function of $U/t$ in the 1D Hubbard model with $N=N_m$. (a) $N=3$, (b) $N=4$, (c) $N=5$.

chirality.[29] If one connects a quantum ring in a perpendicular magnetic field to several leads, features might appear in transport properties.

Finally, we estimate the value of the magnetic field which is necessary to thread the unit flux quantum $\Phi_0$ in a quantum ring. The magnetic field is given by

$$B_0 = \frac{\Phi_0}{\pi r^2} = \frac{\Phi_0}{L^2/(4\pi)},$$

where $r$ and $L$ are the radius and the circumference of the ring, respectively. The unit flux quantum $\Phi_0 = h/e$ amounts to $4.14 \times 10^3$ T nm$^2$. For example, the case of $L=30$ corresponds to about 300 nm (i.e., the radius 48 nm) in GaAs. In this case, we have $B_0 = 0.58$ T, which is a realistic value in the present status.

## V. SUMMARY

We have performed a systematic study of ground-state properties of quantum rings with a few electrons interacting in the form of $1/r$ Coulomb repulsion, using exact diagonalization. For three electrons, the ferromagnetic ground state is uniquely realized when the diameter of the ring is sufficiently large. In contrast, for four and five electrons, the unique ferromagnetic ground state is never realized by the change of the diameter. The results in large rings can be understood in terms of multiple-spin exchanges. When a perpendicular magnetic field is applied to the ring, the persistent current occurs and the spin chirality is finite for a certain value of the flux. The finite spin chirality can also be understood as a result of multiple-spin exchanges in the strong coupling regime.

## ACKNOWLEDGMENTS

The present work is supported by the 21st Century COE program "ORIUM" at Nagoya University from MEXT of Japan. In an early stage of the study, two of the authors (D.S.H. and J.U.) were supported by Casio Science Promotion Foundation.

## APPENDIX: CIRCULARLY ARRANGED QUANTUM DOTS

The confinement potential can vary from parabolic (quantum dot) to ringlike (quantum ring) with use of lithographic techniques.[6–12] In addition, a ring structure can also be fabricated by arraying quantum dots circularly. Although there is a potential energy between the dots, electrons can transfer by tunneling from one dot to another dot. In this case, one may model the array of quantum dots with the tight-binding Hamiltonian. For example, the array of three quantum dots is modeled by the three-site Hubbard model with three electrons. However, the validity of the use of a tight-binding Hamiltonian depends on the size dots.[15] If the size of dots is not too small, the tight-binding description may be valid, because electrons tend to stay within a dot. For small dots, on the other hand, the tight-binding description may not be sufficiently good, and the description in the continuous space would be valid. Here, it is worth clarifying the difference between the continuous model (which has been considered in the main text) and the tight-binding Hamiltonian (i.e., the $N$-site Hubbard model with $N$ electrons). The latter corresponds to the half-filled Hubbard model with a few number of electrons (or sites). Figure 11 shows the lowest energies for each total spin and the energy differences as a function of $U/t$ in the 1D Hubbard model with $N=N_m=3$, 4, and 5. It is found that the relation $E_0(S_{\rm tot}) < E_0(S_{\rm tot}+1)$ always holds for $0 < U/t < \infty$. We note that this relation is the same as the consequence of the Lieb-Mattis theorem,[42] although the theorem is applied to the case of open boundary conditions. For a large but not infinite $U/t$, the Hubbard model at half-filling reduces to the Heisenberg model with antiferromagnetic exchange interaction. For three electrons, the two-spin exchange contributes in the order $O(t^2/U)$, while the multiple-spin exchange does in higher order [e.g., $O(t^3/U^2)$ in the three-cyclic exchange]. This means that the contribution of multiple-spin exchange is very small for a large $U/t$, leading to the relation $E_0(S_{\rm tot}) < E_0(S_{\rm tot}+1)$.

[1] R. C. Ashoori, Nature (London) **379**, 413 (1996).
[2] L. P. Kouwenhoven, D. G. Austing, and S. Tarucha, Rep. Prog. Phys. **64**, 701 (2001).
[3] S. M. Reimann and M. Manninen, Rev. Mod. Phys. **74**, 1283 (2002), and references therein.
[4] A. Lorke, R. J. Luyken, A. O. Govorov, J. P. Kotthaus, J. M. Garcia, and P. M. Petroff, Phys. Rev. Lett. **84**, 2223 (2000).
[5] R. J. Warburton, C. Schäflein, D. Haft, F. Bickel, A. Lorke, K. Karrai, J. M. Garcia, W. Schoenfeld, and P. M. Petroff, Nature (London) **405**, 926 (2000).
[6] T. Heinzel, R. Held, S. Lüscher, K. Ensslin, W. Wegscheider, and M. Bichler, Physica E (Amsterdam) **9**, 84 (2001).
[7] A. Fuhrer, S. Lüscher, T. Ihn, T. Heinzel, K. Ensslin, W. Wegscheider, and M. Bichler, Nature (London) **413**, 822 (2001).
[8] U. F. Keyser, S. Borck, R. J. Haug, M. Bichler, G. Abstreiter, and W. Wegscheider, Semicond. Sci. Technol. **17**, L22 (2002).
[9] A. Fuhrer, A. Dorn, S. Lüscher, T. Heinzel, K. Ensslin, W. Wegscheider, and M. Bichler, Superlattices Microstruct. **31**, 19 (2002).
[10] U. F. Keyser, C. Fühner, S. Borck, R. J. Haug, M. Bichler, G. Abstreiter, and W. Wegscheider, Phys. Rev. Lett. **90**, 196601 (2003).
[11] M. Bayer, M. Korkusinski, P. Hawrylak, T. Gutbrod, M. Michel, and A. Forchel, Phys. Rev. Lett. **90**, 186801 (2003).
[12] A. Fuhrer, T. Ihn, K. Ensslin, W. Wegscheider, and M. Bichler, Phys. Rev. Lett. **91**, 206802 (2003).
[13] S. Viefers, P. Koskinen, P. S. Deo, and M. Manninen, Physica E (Amsterdam) **21**, 1 (2004), and references therein.
[14] Y. Aharonov and D. Bohm, Phys. Rev. **115**, 485 (1959).
[15] J. Usukura, Y. Saiga, and D. S. Hirashima, J. Phys. Soc. Jpn. **74**, 1231 (2005).
[16] C. Herring, Phys. Rev. B **11**, 2056 (1975).

[17] D. J. Thouless, Proc. Phys. Soc. London **86**, 893 (1965).
[18] D. Loss and P. Goldbart, Phys. Rev. B **43**, 13762 (1991).
[19] N. Yu and M. Fowler, Phys. Rev. B **45**, 11795 (1992).
[20] J. F. Weisz, R. Kishore, and F. V. Kusmartsev, Phys. Rev. B **49**, 8126 (1994).
[21] T. Chakraborty and P. Pietiläinen, Phys. Rev. B **50**, 8460 (1994).
[22] Y. M. Liu, C. G. Bao, and T. Y. Shi, Phys. Rev. B **73**, 113313 (2006).
[23] X. G. Wen, F. Wilczek, and A. Zee, Phys. Rev. B **39**, 11413 (1989).
[24] D. S. Rokhsar, Phys. Rev. Lett. **65**, 1506 (1990).
[25] A. J. Schofield, J. M. Wheatley, and T. Xiang, Phys. Rev. B **44**, 8349 (1991).
[26] D. Sen and R. Chitra, Phys. Rev. B **51**, 1922 (1995).
[27] T. Momoi, K. Kubo, and K. Niki, Phys. Rev. Lett. **79**, 2081 (1997).
[28] D. S. Hirashima and K. Kubo, Phys. Rev. B **63**, 125340 (2001).
[29] Y. Taguchi, Y. Oohara, H. Yoshizawa, N. Nagaosa, and Y. Tokura, Science **291**, 2573 (2001).
[30] Y. Saiga and M. Oshikawa, Phys. Rev. Lett. **96**, 036406 (2006); J. Magn. Magn. Mater. (to be published).
[31] V. W. Scarola, K. Park, and S. Das Sarma, Phys. Rev. Lett. **93**, 120503 (2004); V. W. Scarola and S. Das Sarma, Phys. Rev. A **71**, 032340 (2005).
[32] B. Bernu, P. Lecheminant, C. Lhuillier, and L. Pierre, Phys. Rev. B **50**, 10048 (1994).
[33] J.-L. Zhu, S. Hu, Z. Dai, and X. Hu, Phys. Rev. B **72**, 075411 (2005).
[34] F. Malet, M. Barranco, E. Lipparini, R. Mayol, M. Pi, J. I. Climente, and J. Planelles, Phys. Rev. B **73**, 245324 (2006).
[35] M. Aizenman and E. H. Lieb, Phys. Rev. Lett. **65**, 1470 (1990).
[36] For the cases with even-number fermions, wave functions in a region connected by cyclic exchanges cannot be nodeless, because cyclic exchanges of even-number fermions are odd permutations; under odd permutations, fermion wave functions must change the sign.
[37] K. Niemelä, P. Pietiläinen, P. Hyvönen, and T. Chakraborty, Europhys. Lett. **36**, 533 (1996).
[38] Depolarization of electron spins by a magnetic field is observed also in a parabolic confinement potential (i.e., a quantum dot). S. A. Mikhailov and N. A. Savostianova, Phys. Rev. B **66**, 033307 (2002).
[39] Actually, in Figs. 4–6, the value of $\Phi$ was taken in steps of 0.002.
[40] We consider a discretized system. The consequence that the local spin chirality vanishes for $S_{\mathrm{tot}}=S_{\mathrm{max}}$ would hold also in the continuous limit ($N_m \to \infty$).
[41] T. Okamoto and S. Kawaji, Phys. Rev. B **57**, 9097 (1998).
[42] E. Lieb and D. Mattis, Phys. Rev. **125**, 164 (1962).